DOI: https://doi.org/10.24425/amm.2025.154477

D. JOŃCZYK^{1*}

TEMPERATURE DISTRIBUTIONS IN THE CROSS-SECTION OF TIMBER BEAMS REINFORCED WITH VARIOUS STEEL ELEMENTS UNDER CONDITIONS OF HIGH TEMPERATURES

The article presents numerical calculations of the variable heat flow during fire exposure based on the standard fire curve. The aim of the work was to analyse the temperature distributions in cross-sections for various methods of strengthening wooden beams using steel elements glued into the cross-section. Many historic timber elements, where reinforcement was necessary, were repaired using various steel elements. The most common used reinforcements were steel plates and rods glued into the cross-section in various configurations. Historic timber elements are particularly sensitive to fire. Since steel has a high thermal conductivity and timber is a flammable material, an important aspect of steel-reinforced structures is the knowledge of heat flow and, consequently, temperature distributions in the cross-section determining the cross-section combustion rate. In this work, a thermal numerical analysis was carried out in the ANSYS program for six variants of beams reinforced in different configurations with steel elements. The calculation results for the reinforced beams were compared with the unreinforced beam by analysing: temperature distributions in the cross-section, charring depth and charring rate. Based on the calculations, it can be seen that the reinforcement of wooden beams with the use of steel elements does not adversely affect the temperature distributions and charring rate. If properly performed, the reinforcement of wooden beams using steel elements should not increase the risk of faster destruction of the structure during a fire.

Keywords: Fire; temperature distribution; strengthening; historic structures

1. Introduction

Currently, wooden structures are often used in construction due to ecology [1], but over the last few decades it has also been a relatively frequently used construction material especially in small and medium-sized buildings and in the case of the conservation of historic buildings. As with any building material used to make structural elements, sometimes, for various reasons, there is a need to strengthen the structure. Until the wider use of fiber composites for strengthening structures, the most commonly used material was steel [2,3]. The method of using reinforcing steel elements is dictated not only by their strength aspects, but also by their aesthetics, which is especially important when working with historic buildings. There are cases of using wooden elements to enclose a steel cross-section. The wooden enclosure plays an aesthetic role and serves as thermal insulation [4,5]. Wood has a number of beneficial properties, including low weight and resistance to chemical corrosion. The most significant disadvantage from the point of view of using wood as a construction material is its flammability [6]. When designing any structure, in addition to the need to ensure adequate strength, the designer is obliged to ensure adequate fire resistance [7]. Wood, due to its flammability and the fact that its mechanical properties depend on humidity, requires special attention during fire design. During a fire, wood chars, which causes a reduction in the dimensions of the cross-section, and consequently a reduction in strength. Due to the different values of the heat conduction coefficients of wood and steel, combining these two materials in a reinforced structure may affect different rates of cross-section charring. And, due to the change in temperature inside the cross-section, may effect the strength characteristics of the wood. In the literature, one can find studies of both complex wooden structural elements [8], as well as less complicated structures [9,10] and connections [11]. A particularly frequently used tool is numerical modeling, which allows for the analysis of more complicated cases [12], or an extended parametric analysis [13,14]. There are studies analyzing the connections: between wooden elements using steel dowels [15,16], between timber and steel elements [17], between timber elements using dowels and plates [18,19]. In addition, analyses of hybrid steel-wood

^{*} Corresponding author: damian.jonczyk@pcz.pl



CZESTOCHOWA UNIVERSITY OF TECHNOLOGY, FACULTY OF CIVIL ENGINEERING, 19 A. KRAJOWEJ AV., 42-218 CZESTOCHOWA, POLAND

elements are also carried out: CLT wood elements based on steel sections [20,21] and elements attached to the side surface of the steel sections [22]. The paper presents a numerical fire analysis of wooden beams reinforced with aramid fibers [23]. However, there are no studies in the literature analysing the temperature distributions and, consequently, charring of structural wooden elements reinforced with steel elements. The aim of the paper is to analyse the temperature distribution and charring rate in cross-sections of wooden elements reinforced with various steel elements used in different configurations.

2. Materials and methods

The models for calculations were prepared in the Ansys Workbench program. It was assumed that a time-varying thermal analysis would be performed. Thermal and physical material data were assumed based on Eurocode 5 [24] for timber and Eurocode 3 [25] for steel elements. Graphs of values dependent on temperature: specific heat, conductivity and density for timber are presented in Figs. 1-3. The heat flow was analysed in the cross-section plane, therefore isotropic properties were assumed for timber, omitting heat flow along the fibers in the analysis.

Based on the recommendations of Eurocode 1 [26], temperature-time curves are used for the thermal analysis of structural elements simulating fire conditions. The most commonly used

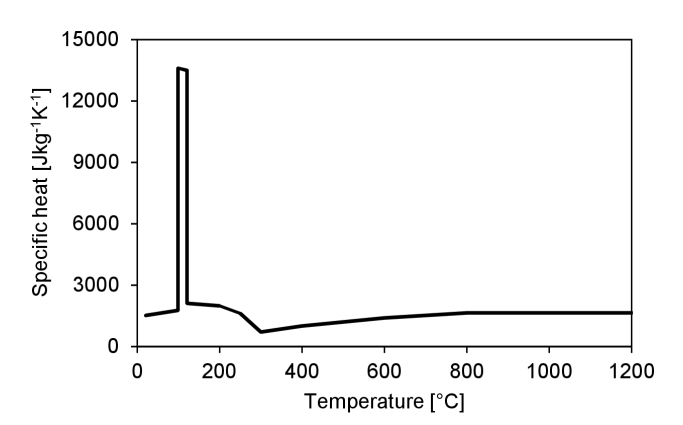


Fig. 1. Specific heat of timber [24]

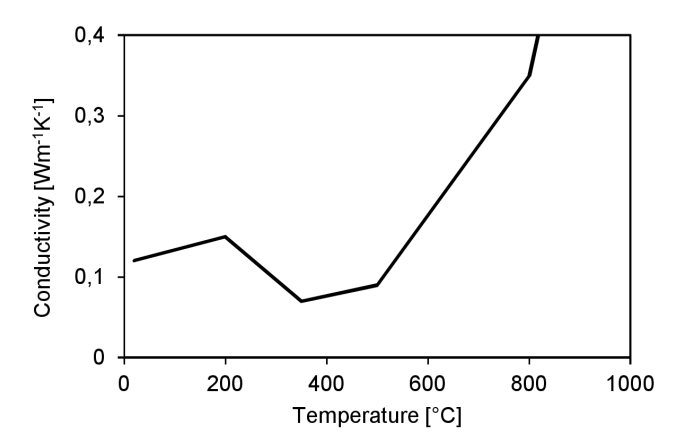


Fig. 2. Thermal conductivity of timber [24]

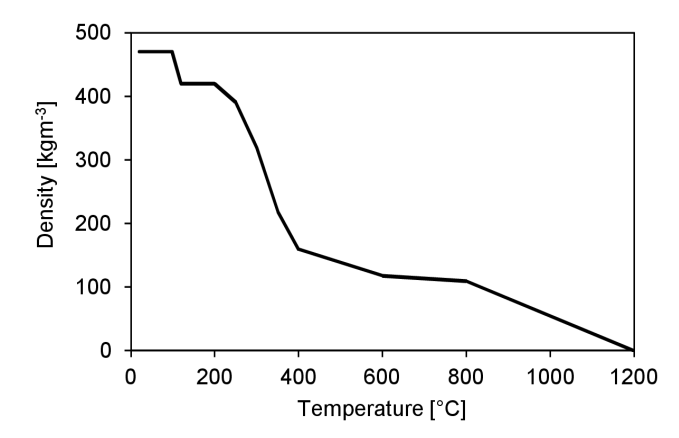


Fig. 3. Timber density [24]

curve in construction is ISO 834 [27] shown in Fig. 4. The temperature increase is described by the function presented in Eq. (1).

$$\Theta_g = 345 \log_{10} (8t + 1) + 20 \tag{1}$$

where Θ_g is the gas temperature during a fire in °C and t is the time in minutes.

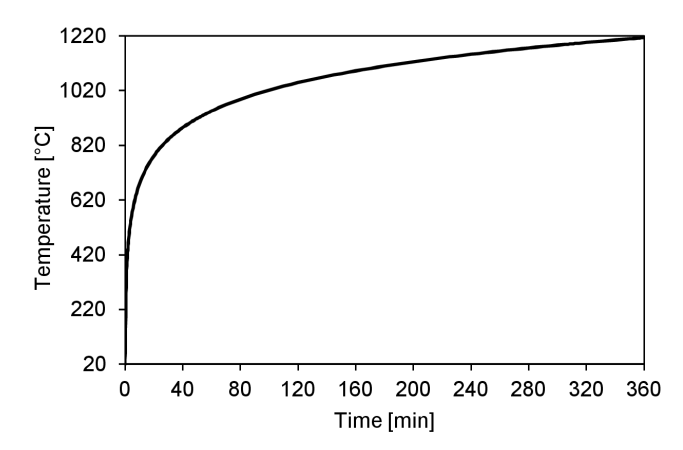


Fig. 4. ISO 834 time-temperature curve [27]

During thermal simulations, Eurocode 5 [24] allows the use of advanced methods, e.g. the Finite Element Method (FEM). High temperature conditions are simulated by assuming the action of the net heat flux on selected edges, presented in the equation Eq. (2), which is composed of two components: the heat flux from convection – Eq. (3) and the heat flux from radiation – Eq. (4).

$$\dot{h}_{net} = \dot{h}_{net,c} + \dot{h}_{net,r} \tag{2}$$

$$\dot{h}_{net,c} = \alpha_c \left(\Theta_g - \Theta_m \right) \tag{3}$$

$$\dot{h}_{net,r} = \Phi \varepsilon_m \varepsilon_f \sigma \left[\left(\Theta_r + 273 \right)^4 - \left(\Theta_m + 273 \right)^4 \right] \tag{4}$$

where α_c is the coefficient of heat transfer by convection in W/m²K equal 25.0, Θ_g is the gas temperature in the vicinity of the fire exposed surface in °C, Θ_m is the surface temperature of the member in °C, Φ is configuration factor equal 1.0, ε_m is the surface emissivity of the member set to 0.8, ε_f is the emissivity of

the fire set to ,1.0, σ is the Stefan-Boltzmann constant in W/m²K⁴ equal 5.67×10⁻⁸, Θ_r is the effective radiation temperature of the fire environment in °C set equal as Θ_g .

Based on the above theoretical assumptions, thermal effects on three edges of the analysed beams were assumed. Geometric models were made in the Space Claim module. The cross-section was modeled in the xy plane appropriate for simulating heat flows in the plane. The analyzed beams used finite elements: SOLID 291, CONTA174 and TARGE170. Since only cases with steel elements glued inside the cross-section were analysed, all contacts were assumed as bonded. The analysis was carefully divided into many calculation steps of different lengths. Due to the large variability of gas temperature over time, the first calculation steps were short and measured in seconds. Then, after flattening the standard curve, the steps were gradually extended. This procedure was used to ensure convergence. The mesh size of all analyzed cross-sections was assumed to be 5 mm. The wooden beam model used in the paper was calibrated based on the experimental tests presented in [28] showing good agreement.

Seven cross-sections made of wood were assumed for the analysis. Six of them were reinforced with various steel elements and one was a comparative wooden cross-section without any reinforcements. The analyzed cross-sections are shown in Fig. 5. The adopted cross-sections were determined based on analyses of scientific literature. The most common reinforcement schemes were used, in which steel elements were located inside the crosssection. This assumption was made due to the requirement to maintain the external aesthetics of the reinforced element. With the exception of series B, in which steel rods with a diameter of 14 mm were used for reinforcement, the remaining series (A, C, D, E, F) were reinforced with 4 mm thick steel plates. The reinforcing plates were positioned horizontally (series A and C) and vertically (series B, D, E, F). The beam from series G was a comparative beam without any reinforcement. All crosssections had the same external dimensions of 100 mm×200 mm. Series F was the only one with reinforcing elements only at the

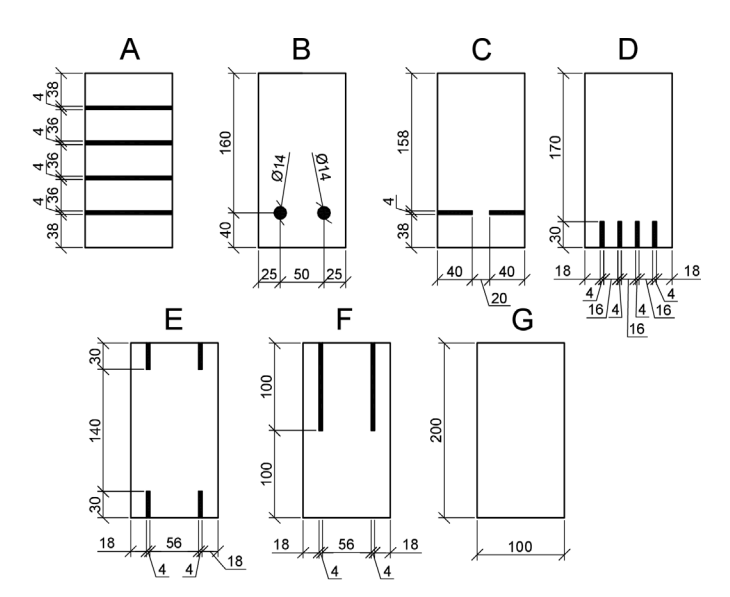


Fig. 5. Models of cross-sections of the analysed beams (dimensions in mm)

upper edges. Series E had reinforcements at the lower and upper surfaces. The remaining series with reinforcements had steel elements at the lower surface.

Based on the assumptions given above, the heat flux acting on the modeled cross-sections was assumed to be convection and radiation. These actions were assumed on three edges as shown in Fig. 6.

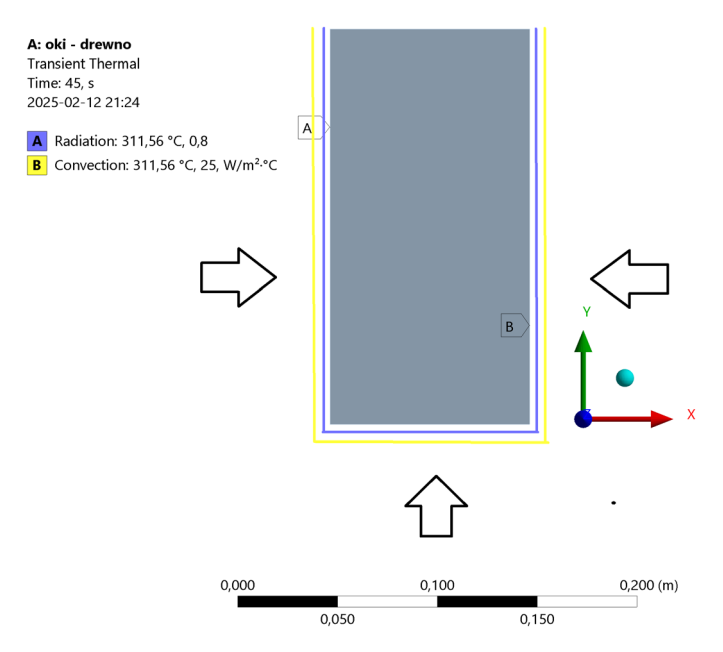


Fig. 6. Boundary conditions

3. Results and discussion

Using the discussed numerical models for all variants of the cross-section, a time-varying thermal analysis was performed. The main goal was to determine the temperature distributions in conditions of elevated temperatures simulating fire conditions. Based on the calculations, the temperature variation over time was determined for two selected points. Two characteristic points were assumed in the middle of the length of the lower edge and the side edge. Both analysed points were assumed at a depth of 10 mm. Fig. 7 shows the temperature variation over time for all analysed cases on the lower horizontal edge of the

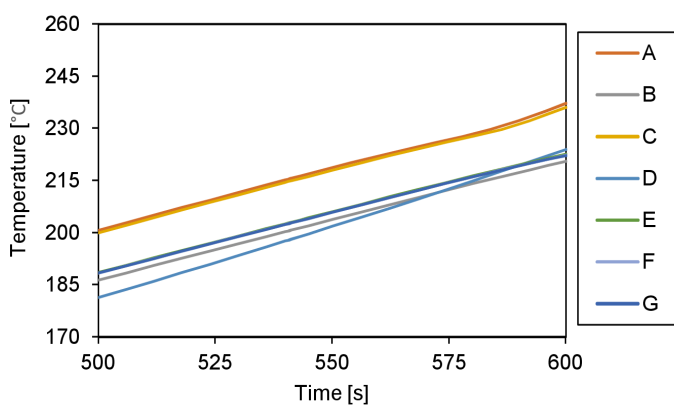


Fig. 7. Time-temperature curve in vertical direction at depth 10 mm

cross-section. It can be seen that during 10 minutes, series A and C were characterized by an increased temperature in relation to the other series. The increase for both series was similar and amounted to about 6% in relation to the other cross-sections.

Fig. 8 shows the temperature increase as a function of time at the mid-height of the side edge of the cross-section. In contrast to the data from Fig. 7, higher temperatures were recorded for series D, E and F, while the lowest temperature was recorded for series A. The highest temperature increase occurred for series E and, in comparison to the unreinforced beam of series G, it amounted to 13%. TABLE 1 shows the temperature distributions for all analysed cross-sections at 2.5, 5 and 10 minutes of exposure to elevated temperatures. Based on

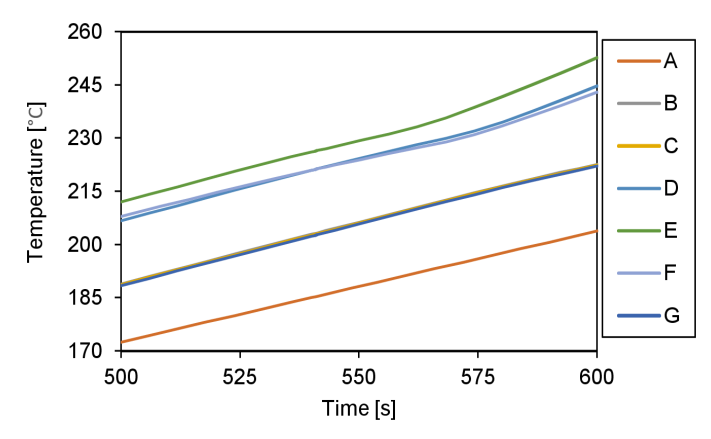


Fig. 8. Time-temperature curve in horizontal direction at depth 10 mm

TABLE 1 Temperature distributions in analysed beams

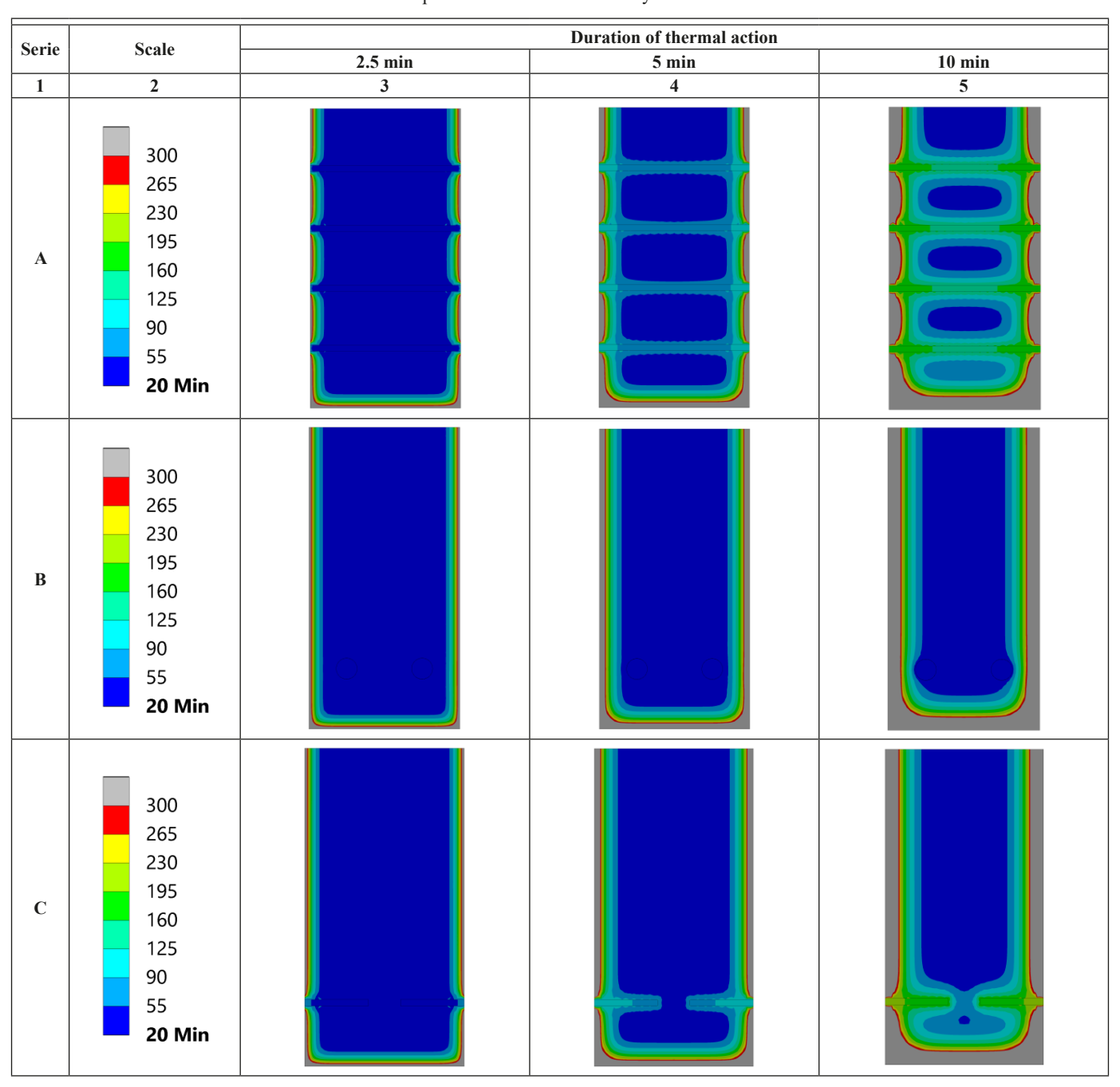
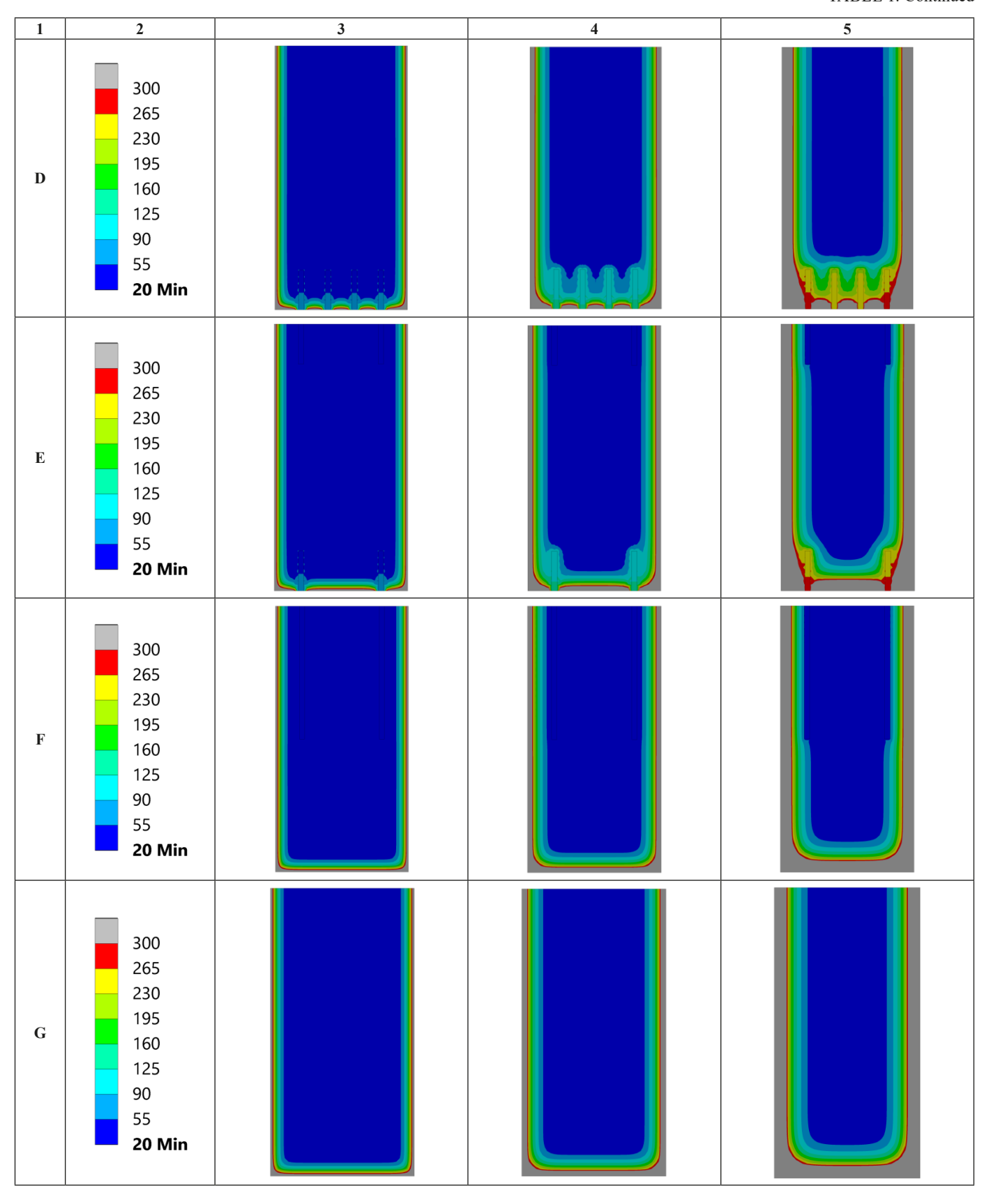


TABLE 1. Continued



the assumptions of Eurocode 5 [24], it was assumed that above the 300° C isotherm, wood charring occurred, therefore these areas were marked in grey. The greatest charring of the corners of cross-sections can be seen in series D and E.

On the basis of measurements in two directions for a time of 10 mins, the charring rates were also determined for both directions. Charring rates were determined based on the relationship (5) presented in TABLE 2

$$d_{char.i} = t \,\beta_i \tag{5}$$

where $d_{char,i}$ is charring depth in mm (x – horizontal direction, y – vertical direction), t is time of fire exposure in min set as 10 min and β_i is charring rate (x – horizontal direction, y – vertical direction).

 $\label{eq:table 2} TABLE\ 2$ Charring rate and charring depth after fire-exposure time of 10 min

Serie	$d_{char,x}$	$d_{char,y}$	Charring rate	
			β_x	β_y
	[mm]	[mm]	[mm/min]	[mm/min]
A	7.7	8.3	0.77	0.83
В	8.3	8.3	0.83	0.83
C	8.4	8.3	0.84	0.83
D	8.2	6.9	0.82	0.69
Е	8.2	8.4	0.82	0.84
F	8.0	8.4	0.80	0.84
G	8.3	8.3	0.83	0.83

There is no significant difference in the charring rates for all series (TABLE 2). Apart from two deviations of 7% in the horizontal direction and 17% (lower rate in reinforced elements) in the vertical direction for the reinforced beams with respect to the unreinforced beam. The remaining values did not differ by more than 1% with respect to the unreinforced beam.

4. Conclusions

The article analyses temperature distributions in crosssections of wood reinforced with steel elements subjected to elevated temperatures. Seven variants of cross-sections were analysed. Six of them were reinforced with various steel elements, while one was a comparative, unreinforced cross-section.

Based on the calculations and analyses carried out, the following conclusions can be drawn:

- Reinforcing the cross-sections of wood with steel elements does not significantly affect the temperature distributions and, consequently, the cross-section charring rate.
- The cross-section charring coefficient differs on average by about 2% between the unreinforced beam and the reinforced beams, to the advantage of the reinforced beams.
- The temperature increase in the analysed series was not significant and amounted to about 10%.
- Analysing the temperature increases in the individual series, it can be seen that steel elements affect local temperature values, especially in a situation where steel elements located parallel to the aforementioned edge are close to the heated edge.
- Based on the temperature maps, it can be seen that vertically mounted steel elements heat up, increasing the temperature in their immediate vicinity while blocking the free flow of heat into the cross-section, which can have a beneficial effect on the depth of charring.

Many historic buildings have structural elements made of wood and in cases of structural wear or design and construction errors, there was a need to reinforce the structure. Until the appearance of fibre composites, steel elements were most often used for reinforcement. Currently, hybrid wood-steel elements are also used, which is why it is important to know the behaviour of such elements during a fire. Since wood is a flammable material, it is particularly important in this case.

In the case where steel reinforcements are needed, their effect on the temperature distributions and, consequently, the rate of cross-section charring should be analysed individually depending on the location of the places necessary for reinforcement.

Acknowledgement

The authors would like to express their gratitude for providing access to the computing infrastructure built in the projects No. POIG.02.03.00-00-028/08 "PLATON – Science Services Platform" and No. POIG.02.03.00-00-110/13 "Deploying high-availability, critical services in Metropolitan Area Networks (MAN-HA)".

REFERENCES

- [1] A. Mishra, F. Humpenöder, G. Churkina et al., Land use change and carbon emissions of a transformation to timber cities. Nat Commun 13, 4889 (2022).
 - DOI: https://doi.org/10.1038/s41467-022-32244-w
- [2] J. Jasieńko, T.P. Nowak, Solid timber beams strengthened with steel plates Experimental studies. Construction and Building Materials **63**, 81-88 (2014).
 - DOI: https://doi.org/10.1016/j.conbuildmat.20d14.04.020
- [3] A. Borri, M. Corradi, Strengthening of timber beams with high strength steel cords. Composites Part B: Engineering 42 (6), 1480-1491 (2011).
 - DOI: https://doi.org/10.1016/j.compositesb.2011.04.051
- [4] S. Šulc, J. Šejna, V. Šmilauer, F. Wald, Steel elements with timber fire protection - experiment and numerical analysis. Acta Polytechnica CTU Proceedings 34, 116-121 (2022).
 - DOI: https://doi.org/10.14311/APP.2022.34.0116
- [5] M. H. Nguyen, S.E. Ouldboukhitine, S. Durif, V. Saulnier, A. Bouchair, Passive fire protection of steel profiles using wood. Engineering Structures 275 (A), 115274 (2023). DOI: https://doi.org/10.1016/j.engstruct.2022.115274
- [6] V.D. Thi, M. Khelifa, M. El Ganaoui, Y. Rogaume, Finite element modelling of the pyrolysis of wet wood subjected to fire. Fire Safety Journal **81**, 85-96 (2016).
 - DOI: https://doi.org/10.1016/j.firesaf.2016.02.001
- [7] E. Garcia-Castillo, I. Paya-Zaforteza, A. Hospitaler, Fire in heritage and historic buildings, a major challenge for the 21st century. Developments in the Built Environment 13, 100102 (2023). DOI: https://doi.org/10.1016/j.dibe.2022.100102

- [8] E. Garcia-Castillo, I. Paya-Zaforteza, A. Hospitaler, Analysis of the fire resistance of timber jack arch flooring systems used in historical buildings. Engineering Structures 243, 112679 (2021). DOI: https://doi.org/10.1016/j.engstruct.2021.112679
- [9] B. Chorlton, J. Gales, Fire performance of heritage and contemporary timber encapsulation materials. Journal of Building Engineering 29, 101181 (2020).
 DOI: https://doi.org/10.1016/j.jobe.2020.101181
- [10] T. Gernay, Fire resistance and burnout resistance of timber columns. Fire Safety Journal 122, 103350 (2021).
 DOI: https://doi.org/10.1016/j.firesaf.2021.103350.
- [11] R. Regueira, M. Guaita, Numerical simulation of the fire behaviour of timber dovetail connections. Fire Safety Journal 96, 1-12 (2018). DOI: https://doi.org/10.1016/j.firesaf.2017.12.005
- [12] P.A.G. Piloto, D. Vergara, Light timber framed wall under fire: Effect of the load and cladding. Engineering Structures 280, 115696 (2023). DOI: https://doi.org/10.1016/j.engstruct.2023.115696
- [13] J. Shin, H. Lee, I.R. Choi et al., Fire performance of CFRP-strengthened piloti-type columns with fire-resistant materials during standard fire exposure. Sci Rep 14, 23597 (2024). DOI: https://doi.org/10.1038/s41598-024-74306-7
- [14] T. Han, S. Tesfamariam, Reliability analysis of timber columns under fire load using numerical models with equivalent section temperature. Engineering Structures 324, 119345 (2025). DOI: https://doi.org/10.1016/j.engstruct.2024.119345
- [15] A. Szász, V. Hlavička, É. Lublóy, A. Biró, Numerical modelling of the fire resistance of double sheared steel-to-timber connections. Journal of Building Engineering 37, 102150 (2021). DOI: https://doi.org/10.1016/j.jobe.2021.102150
- [16] P. Palma, A. Frangi, Modelling the fire resistance of steel-to-timber dowelled connections loaded perpendicularly to the grain. Fire Safety Journal 107, 54-74 (2019). DOI: https://doi.org/10.1016/j.firesaf.2017.12.001
- [17] M. Audebert, D. Dhima, M. Taazount, A. Bouchaïr, Experimental and numerical analysis of timber connections in tension perpendicular to grain in fire. Fire Safety Journal 63, 125-137 (2014), DOI: https://doi.org/10.1016/j.firesaf.2013.11.011

- [18] C. Gomes, E.M.M. Fonseca, H.M. Lopes, Thermomechanical Analysis of Steel-to-Timber Connections under Fire and the Material Density Effect. Appl. Sci. 12, 10516 (2022). DOI: https://doi.org/10.3390/app122010516
- [19] M. Khelifa, V.D. Thi, M. Oudjène et al., Modelling the Response of Timber Beams Under Fire. Int J Civ Eng 22, 1537-1549 (2024). DOI: https://doi.org/10.1007/s40999-024-00973-2
- [20] M.G. Dellepiani, G.R. Munoz, S.J. Yanez, C.F. Guzmán, E.I.S. Flores, J.C. Pina, Numerical study of the thermo-mechanical behavior of steel-timber structures exposed to fire. Journal of Building Engineering 65, 105758 (2023).
 DOI: https://doi.org/10.1016/j.jobe.2022.105758
- [21] A. Jeebodh, B. Davison, M.S. McLaggan, I. Burgess, D. Hopkin, S.-S. Huang, Influence of continuous elastic lateral restraints on beams and beam-columns of steel-timber hybrid structures in fire. Fire Safety Journal 146, 104172 (2024). DOI: https://doi.org/10.1016/j.firesaf.2024.104172
- [22] M. Malaska, M. Alanen, M. Salminen et al., Fire Performance of Steel-Timber Hybrid Beam Section. Fire Technol 60, 2581-2600 (2024). DOI: https://doi.org/10.1007/s10694-023-01471-y
- [23] D. Jończyk, D. Hajdas, M. Major, Numerical analysis of temperature distributions in glulam beams exposed to fire and reinforced with aramid composite. ZN SGSP 91 (1), 7-21 (2024). DOI: https://doi.org/10.5604/01.3001.0054.7280
- [24] EN 1995-1-2 Eurocode 5: Design of timber structures Part 1-2: General Structural fire design.
- [25] EN 1993-1-2 Eurocode 3: Design of steel structures Part 1-2: General rules Structural fire design
- [26] EN 1991-1-2 Eurocode 1: Actions on structures Part 1-2: General actions Actions on structures exposed to fire.
- [27] ISO 834-1:1999 Fire-resistance tests Elements of building construction Part 1: General requirements.
- [28] L. Kucíková, T. Janda, J. Sykora, M. Šejnoha, G. Marseglia, Experimental and numerical investigation of the response of GLT beams exposed to fire. Construction and Building Materials 299, 123846 (2021).
 - DOI: https://doi.org/10.1016/j.rcns.2025.02.004